

Equilibrium Study of Complex Formation Among Trivalent Metals, Glycine Peptides and Phenolates in Aqueous Solution

Artik Elisa Angkawijaya¹ · Shella Permatasari Santoso¹ ·
Felycia Edi Soetaredjo² · Suryadi Ismadji² · Yi-Hsu Ju²

Received: 28 October 2014 / Accepted: 30 June 2015 / Published online: 20 October 2015
© Springer Science+Business Media New York 2015

Abstract The stability of binary and mixed-ligand complexes among trivalent transition metal ions (chromium and iron), glycine peptides (glycylglycine and glycylglycylglycine) and phenolates (ferulic acid and gallic acid) were studied by using pH-potentiometric titration in aqueous solution at 298.15 K and ionic strength of 0.15 mol·dm⁻³ NaNO₃. The complexation model for each system was obtained by processing the potentiometric titration data using the HYPERQUAD2008 program. The stability constant trend of complexes in both systems and the contributions of deprotonated or protonated amide peptides to the stability of the complexes is discussed. The stability of the mixed-ligand complexes relative to their corresponding binary complexes was also investigated by calculating the $\Delta\log_{10} K$ parameter of each system. In addition, the Gibbs energies of reaction ($\Delta_r G$) obtained from the Gaussian modeling program with B3LYP/6-31+G(d) basis set were used to verify the contributing binding sites of the ligands and to predict the structures of the M–L complexes.

Keywords Solution equilibria · Peptides · Phenolates · Potentiometry · Gaussian

Abbreviations

| | |
|-----|------------------|
| Gp | Glycine peptides |
| G | Glycine |
| GG | Diglycine |
| GGG | Triglycine |
| Ph | Phenolates |
| FA | Ferulic acid |
| GA | Gallic acid |

✉ Yi-Hsu Ju
yhju@mail.ntust.edu.tw

¹ Chemical Engineering Department, National Taiwan University of Science and Technology, Taipei 106-07, Taiwan

² Chemical Engineering Department, Widya Mandala Catholic University, Surabaya 60114, Indonesia

1 Introduction

In living cells tissues, chromium (Cr^{3+}) and iron (Fe^{3+}) are essential micronutrients. In particular, iron is needed for transporting oxygen to tissues and for developing new cells in the human body while chromium is essential for lipid, protein, and fat metabolisms in animals and humans and is used to potentiate insulin activity in peripheral tissue. However, excessive uptake of these metals may affect human leukocytes, trigger carcinogenesis and cause clastogenesis for human leukocytes [1–4]. In more severe conditions, iron also may cause fatal cell death and tissue injury due to its ability to catalyze the generation of free radicals [5–7]. Chelation therapy is a well-known and efficacious treatment for patients with metal poisoning [8–10]. This treatment uses metal–ligand coordination principle, in which the chelating agent acts as a ligand that will bind metal ions and form a metal ligand complex so that these excess toxic metals can be excreted from the human body in their complexed form.

Study of the chelating ability of glycine peptides (Gp), in particular diglycine (GG) and triglycine (GGG), with some divalent metal ions (Co^{2+} , Ni^{2+} and Cu^{2+}) has shown that glycine peptides are potential metal chelators via their amine and carboxyl functional groups [11]. For GG and GGG, the occurrence of an amide bond in its backbone may also effect the stability of the formed complex. It has been shown that acid deprotonation constant of an amide nitrogen in the absence of metal ions is very high ($\text{p}K_{\text{a}} \sim 15$), but administration of divalent copper or nickel is able to reduce the proton ionization constant to a $\text{p}K_{\text{a}}$ of 4–8, which is experimentally and biologically accessible for further use as an additional chelating binding site [12].

Phenolates (Ph) can act as reducing agents, as hydrogen atom-donating antioxidants, and metal chelators [13], thereby reducing the metal's capacity to generate free radicals [14, 15]. Ferulic acid (FA) and gallic acid (GA) are two common phenolates that naturally exist in plants. Both FA and GA are remarkable antioxidants and more efficient in preventing free radical oxidation than vitamin C [14–22]. The antioxidant potential of FA is caused by the occurrence of the phenolic nucleus and unsaturated side chain that can readily form a resonance stabilized phenoxy radical. FA is a potential metal chelator through its carboxyl and phenol groups [14, 23] while GA is coordinated to the metal ion through its three hydroxyl groups and one carboxyl group. A study of the activity of GA against hepatitis induced cancer suggested that the cytotoxicity of three adjacent hydroxyl groups and carboxyl group of GA makes it selective for killing cancer cells without harmful effects to normal cells [24].

Both peptides (GG and GGG) and phenolates (FA and GA) were used in this work to study their complexing ability with two trivalent metals (Cr^{3+} and Fe^{3+}). The formation constants of these complexes in binary and mixed-ligand systems were determined by using the pH-potentiometric method at 298.15 K and an ionic strength of $0.15 \text{ mol}\cdot\text{dm}^{-3}$ NaNO_3 , which is the ionic strength of most body fluids. Moreover, DFT calculations by the Gaussian 09W program were used to confirm the contributing binding site of the ligand, predict the structure and calculate the Gibbs energy of reaction ($\Delta_r G$) [25].

2 Experimental Section

2.1 Chemicals Used

Ferric nitrate nonahydrate ($\text{Fe}(\text{NO}_3)_3 \cdot 9\text{H}_2\text{O}$, 98 % purity) and chromium chloride hexahydrate ($\text{CrCl}_3 \cdot 6\text{H}_2\text{O}$, 98 % purity) were purchased from Across Organics (Morris Plains,

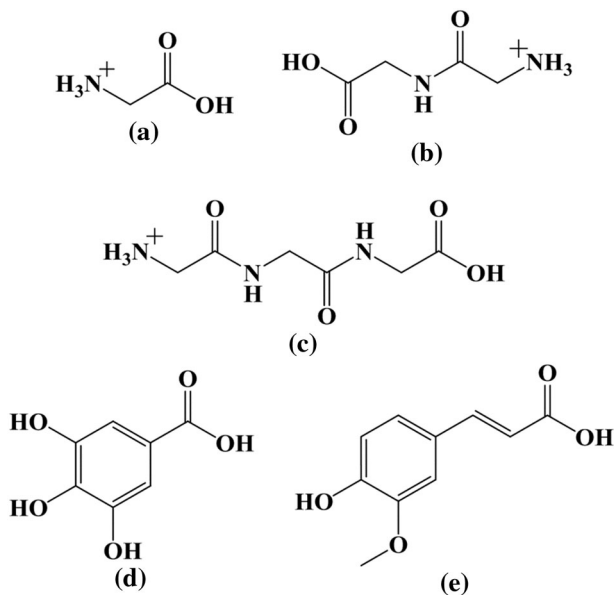


Fig. 1 Structural formulae of **a** glycine, **b** glycylglycine, **c** glycylglycylglycine, **d** gallic acid and **e** ferulic acid

NJ). Both of the metal salts were standardized against ethylenediaminetetraacetic acid (EDTA, 99.95 % purity), which was purchased from Sigma–Aldrich (Steinheim, Germany). The ligands used in this study were purchased from Sigma–Aldrich (Steinheim, Germany) (G, 99.7 % purity; GG, 99 % purity; GGG, 99 % purity; GA, 99 % purity and FA, 99 % purity); their structures are shown in Fig. 1.

Nitric acid (Panreac, Barcelona, Spain; purity 65 %) solution, for acidifying the solutions for determination of stability constants, was prepared and standardized prior to use. Before using it as a titrant, carbonate-free sodium hydroxide (NaOH) from Across Organics (Morris Plains, NJ) was standardized against potassium hydrogen phthalate (KHP, 99.95 % purity) from Sigma–Aldrich (Steinheim, Germany). To maintain ionic strength in the solutions, sodium nitrate (NaNO_3 , 99 % purity) from Across Organics (Morris Plains, NJ) was used. All chemicals used in this study were of analytical grade and were used without further purification. Solutions were prepared daily in distilled deionized water (resistance 18.3 $\text{M}\Omega\cdot\text{cm}$).

2.2 Potentiometric Titration

Prior to the measurements, the following solutions were prepared (total volume 50 cm^3) and were titrated potentiometrically against standard carbonate-free NaOH (0.10 mol dm^{-3}):

- 5 mL of 0.03 $\text{mol}\cdot\text{dm}^{-3}$ HNO_3 + 10 mL of 0.75 $\text{mol}\cdot\text{dm}^{-3}$ NaNO_3
- solution (a) + 5–6 mL of 0.01 $\text{mol}\cdot\text{dm}^{-3}$ ligand + 2–5 mL of 0.01 $\text{mol}\cdot\text{dm}^{-3}$ metal ion
- solution (a) + 5 mL of 0.01 $\text{mol}\cdot\text{dm}^{-3}$ metal ion + 5 mL of 0.01 $\text{mol}\cdot\text{dm}^{-3}$ ligand Gp + 5 mL of 0.01 $\text{mol}\cdot\text{dm}^{-3}$ ligand Ph

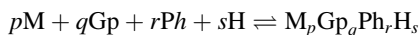
Solution (b) was prepared at four different metal-to-ligand concentration ratios (1:1, 1:2, 1:2.5 and 1:3). All of the titrations were carried out in a 100 cm³ double-walled equilibrium cell that was connected to a refrigerated circulating bath to maintain the temperature of the reagents at 298.15 ± 0.1 K. Each titration was repeated at least three times in the pH range 2.5–11 with a reproducibility of ± 0.02 in pH unit.

The potentiometric titrations were performed using a Metrohm 702 SM titrino, equipped with a 649 magnetic stirrer and a Dosino burette (model 683) and coupled with an Ecotrode plus pH glass electrode. Electrode response can be read to the third decimal place in pH units with a readability of ± 0.001 . Since the determination of metal–ligand stability constants were carried out in high ionic strength of 0.15 mol·dm⁻³ NaNO₃ ($pK_w = 13.77$ at the given ionic strength and temperature), it is necessary carry out a strong acid–strong base titration for the glass electrode calibration. For this purpose, the titration curves of solution (a) were processed by using the Glass Electrode Evaluation program (GLEE) to calibrate the glass electrode in terms of hydrogen ion concentration [26]. While the titration curve of solution (a) was used in the electrode calibration, titration curves of solutions (b) and (c) were employed in determining complex formation constants in binary and mixed-ligand systems, respectively.

2.3 Data Analysis

The calculations were performed using the computer program HYPERQUAD2008 by inputting the titration data. These data were obtained as volume of the base added versus the pH value, and were used for calculations without the need to convert into hydrogen ion concentrations. The stoichiometry and stability constants of the complexes formed were determined by testing various possible composition models. The model selected gave the best statistical fit and was chemically consistent with the titration data without giving any systematic drifts in the various residuals.

The stability constants are presented as the overall formation constant (β_{pqrs}) with stoichiometric coefficient p, q, r, s that represent metal ions, glycine peptides, phenolates and hydrogen atoms, respectively. The formation constant is a function of the complex species concentration $[M_p G_p q Ph_r H_s]$ and free reactant concentrations $[M], [Gp], [Ph]$ and $[H]$, and is expressed by the equation below:



$$\beta_{pqrs} = \frac{[M_p G_p q Ph_r H_s]}{[M]^p [Gp]^q [Ph]^r [H]^s}$$

A larger value of the stability constant ($\log_{10}\beta$) indicates that the complex is more stable. The larger is the $\log_{10}\beta$ value, the greater is the driving force to push the reaction to the right side [27]. In addition, the speciation diagrams of the metal–ligand complexes, based on their concentration at certain pH, are calculated by using the HySS2009 program.

2.4 Gaussian Structure Prediction

In this work, the Gaussian 09 program was used to predict the binding site of the ligands that contribute to complex formation and the structure of the complexes [25]. The model structures of these complexes were optimized using density functional theory (DFT) with Becke's three-parameter hybrid method combined with Lee–Yang–Parr correlation

function (B3LYP) [28, 29]. For the basis set, 6-31G with diffuse and polarization functions (+d) was used [30–32]. Along with geometry optimization, frequency analysis was done to obtain the thermochemical properties of the complexes. The B3LYP/6-31+G(d) basis set was chosen since it has been shown to be a suitable basis set for analysis of the molecular orbitals of metal complexes [30–34]. Some simplifications adopted from previous work were employed in this modeling study [35]. The validity of the structure optimization was checked by using normal-mode frequency analysis, in which the real minimum structure must exhibit positive value for all frequencies.

3 Result and Discussion

Protonation constants (pK_a) for glycine (G), glycine peptides (GG and GGG) and phenolates (FA and GA) at 298.15 K and ionic strength $0.15 \text{ mol}\cdot\text{dm}^{-3}$ NaNO_3 have been reported in some previous work [35–37]. The pK_a s of the carboxyl group of G, GG and GGG are 2.32, 3.21 and 3.30 while for the amine group are 9.62, 8.31 and 7.90, respectively [35]. The pK_a s of the phenolate FA are 4.46 for the carboxyl group and 8.82 for its hydroxyl group [37]. For GA, the pK_a of the carboxyl group is 4.25, followed by the protonation of the hydroxyl group at the *para* position with $pK_a = 8.61$ and the two hydroxyl groups at the *meta* position with pK_a s of 11.03 and 12.71 [36]. These protonation constants were entered into the HYPERQUAD2008 program for determination of the metal complexes' stability constants. By considering the hydrolysis reaction of the metal ions, the metal hydrolysis constants for $[\text{M}(\text{OH})]^{2+}$, $[\text{M}(\text{OH})_2]^+$ and $[\text{M}(\text{OH})_3]$ were also included in the determination of stability constants, which for Cr^{3+} are -4.00 , -5.70 and -8.30 , while for Fe^{3+} are -2.19 , -3.48 and -6.33 , respectively [38].

3.1 Complex Formation Between Trivalent Metal Ions and Glycine Peptides

For determination of metal complex formation constant ($\log_{10}\beta$), the prepared solution (c) that consists of metal and ligand in various molar ratios (1:1, 1:2, 1:2.5 and 1:3) was titrated against carbonate-free sodium hydroxide solution. Stability constants of the metal ion (Cr^{3+} and Fe^{3+}) complexes with Gp (GG and GGG) are expressed as the logarithm of the overall formation constant ($\log_{10}\beta$). As presented in Table 1, the stability of the complexes containing Fe^{3+} are larger than those containing Cr^{3+} and this phenomenon was observed regardless of the peptide used ($\log_{10}\beta_{\text{FeGG}} = 8.62 > \log_{10}\beta_{\text{CrGG}} = 7.18$; $\log_{10}\beta_{\text{FeGGG}} = 8.38 > \log_{10}\beta_{\text{CrGGG}} = 7.15$). This might be due to the increasing charge density in going from Cr to Fe (for a given ligand and trivalent metal ion). Fe^{3+} has a higher charge density since it has a smaller ionic radius than Cr^{3+} , thus allowing ligand to bind the central metal atom easier and form more stable metal complexes [39]. The Gibbs energy (G) values of free Cr^{3+} and Fe^{3+} ions also support this order, where Fe^{3+} has a more negative value (-1262.752 hartree/particle) than that of Cr^{3+} (-1043.655 hartree/particle), which indicates that Fe has a higher ionization energy than Cr; thus the complexes of Fe^{3+} will have higher stability.

Glycine ($\log_{10}\beta_{\text{FeG}} = 10.69$) was found to form a more stable metal complex compared to diglycine ($\log_{10}\beta_{\text{FeGG}} = 8.62$) and triglycine ($\log_{10}\beta_{\text{FeGGG}} = 8.38$). This can be explained by the structure of the ligands. The smallest and simplest ligand glycine can form five-membered ring complexes with metal ions via the amine and carboxyl groups. On the other hand, for GG and GGG, since the N-terminus and C-terminus are at greater distance (longer chain length) than that of ligand G, thus the formed metal complexes will have a larger ring structure resulting in less stable metal complexes [12].

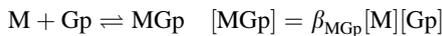
Table 1 Overall formation constants of trivalent metal ion (M)–glycine peptide (Gp) complexes at 298.15 K and 0.15 mol·dm⁻³ NaNO₃

| Species | log ₁₀ β ± S.D. | | |
|--|-----------------------------------|--------------|--------------|
| | Gp = G | Gp = GG | Gp = GGG |
| M = Fe ³⁺ | | | |
| σ* ^b | 1.155 | 1.156 | 1.093 |
| [MGp] ²⁺ | 10.69 ± 0.09 (10.83) ^a | 8.62 ± 0.06 | 8.38 ± 0.06 |
| [MGpH ₋₁] ⁺ | 7.28 ± 0.08 | 5.77 ± 0.06 | 5.57 ± 0.03 |
| [MGpH ₋₂] | 3.56 ± 0.07 | | 1.97 ± 0.03 |
| [MGp ₂] ⁺ | 20.42 ± 0.05 (20.48) ^a | | |
| [MGp ₂ H ₋₂] ⁻ | | 5.63 ± 0.06 | 5.07 ± 0.06 |
| [MGp ₃] | 30.08 ± 0.07 | | |
| M = Cr ³⁺ | | | |
| σ* ^b | 1.338 | 1.052 | 1.047 |
| [MGp] ²⁺ | 8.77 ± 0.04 | 7.18 ± 0.02 | 7.15 ± 0.02 |
| [MGpH ₋₁] ⁺ | 2.42 ± 0.06 | 1.34 ± 0.06 | 0.88 ± 0.09 |
| [MGpH ₋₂] | -3.60 ± 0.04 | | -4.20 ± 0.03 |
| [MGp ₂] ⁺ | 15.74 ± 0.03 | | 12.19 ± 0.05 |
| [MGp ₂ H ₋₁] | | 6.88 ± 0.03 | 5.92 ± 0.04 |
| [MGp ₂ H ₋₂] ⁻ | | -0.35 ± 0.03 | -1.34 ± 0.04 |
| [MGp ₃] | 21.73 ± 0.09 | | |

^a Ref. [49], *T* = 298.15 K, *I* = 0.1 mol·dm⁻³ NaNO₃

^b Sigma* (σ*) is the goodness of fit for a system with ±95 % probability

A peptide offers one or more amide groups and a carbonyl group as the binding sites in addition to the amine (N-terminus) and carboxyl (C-terminus) groups. The amide group is a very weak acid and tends to remain neutral throughout most of the pH range; this causes difficulty for H atom deprotonation from the trigonal nitrogen to yield a negatively charged ligand. Because of the neutrality of the amide group, the amine and carboxyl groups are more effective as binding sites. The presence of metal ions enables the amide group to deprotonate easier and also enables the amide group to participate in complex coordination. These factors were also mentioned in some studies where the amide groups were also capable of coordinating with metal ions in solution [12, 40–42] and coordination of the amide group occurred after deprotonation. Thus, in this study, the influences of protonated and deprotonated amide nitrogens in peptide bonds on the stability of complex species were compared and investigated by the following expressions:



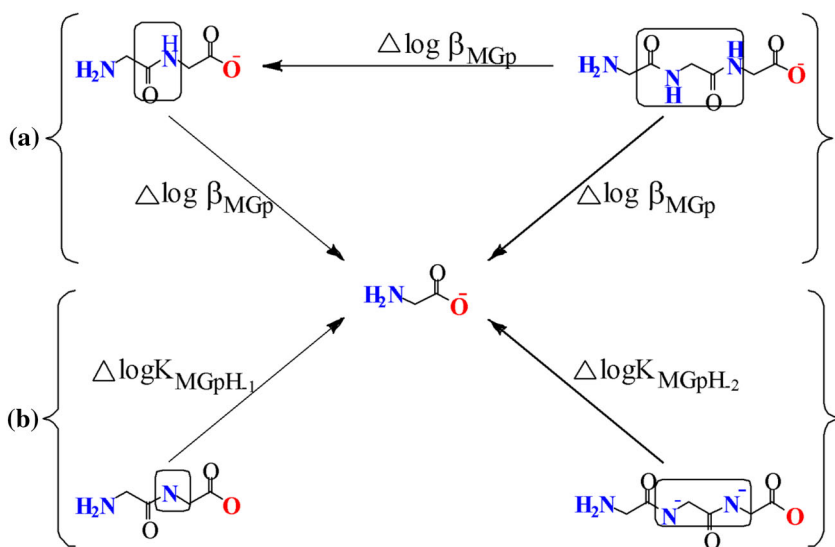


where a negative value of H refers to deprotonation of the amide group in metal complexes.

For example, $[\text{M}(\text{Gp}, \text{H}_{-1})]$ in the system containing diglycine refers to the formation of a complex between metal ion with this ligand in its deprotonated amide form $[\text{GGH}_{-1}]$. As illustrated in Scheme 1, subtraction of $\log_{10}\beta_{\text{MGp}}$ from $\log_{10}\beta_{\text{MGG}}$ and $\log_{10}\beta_{\text{MGGG}}$, as well as subtraction of $\log_{10}\beta_{\text{MGG}}$ from $\log_{10}\beta_{\text{MGGG}}$, were carried out to evaluate the effect of the un-deprotonated amide nitrogen peptide bond on complex stability. Similarly, subtractions of $\log_{10}K_{\text{M}(\text{Gp}, \text{H}_{-1})}$ and $\log_{10}K_{\text{M}(\text{Gp}, \text{H}_{-2})}$ of G from those for of GG and GGG, respectively, were done to evaluate the impact of amide nitrogen deprotonation on the stability of metal complexes.

The subtracted values of $\log_{10}\beta_{\text{MGp}}$ are listed in Table 2. Negative values indicate the absence of participation of a protonated amide nitrogen. The negative value of $\Delta\log_{10}\beta_{\text{MGp}}$ is also possibly due to participation of the amide nitrogen with a lower electron density than amine nitrogen. It is interesting to note that the $\Delta\log_{10}\beta_{\text{MGp}}$ values of metal complexes involving GG and GGG are very small (-0.24 for the Fe^{3+} system and -0.03 for the Cr^{3+} system) while the subtracted values of $\log_{10}\beta_{\text{MP}}$ of GG-G and GGG-G vary from -1.59 to -2.31 . The small $\Delta\log_{10}\beta_{\text{MGp}}$ values of GGG-GG are due to the backbone length of GGG which causing a steric effect [43, 44]. But, since GG and GGG form chelates in the same manner, the stability constants of the complexes formed are also similar.

In Table 2, subtraction of $\log_{10}K_{\text{M}(\text{Gp}, \text{H}_{-1})}$ of GG from $\log_{10}K_{\text{M}(\text{Gp}, \text{H}_{-1})}$ of G and subtraction of $\log_{10}K_{\text{M}(\text{Gp}, \text{H}_{-2})}$ of GGG from $\log_{10}K_{\text{M}(\text{Gp}, \text{H}_{-2})}$ of G both yield positive values. These results indicate that the deprotonated amide nitrogen participated in the complex formation reaction of the metal ions. Moreover, it also shows that $\Delta\log_{10}K_{\text{M}(\text{Gp}, \text{H}_{-2})}$ is more positive than $\Delta\log_{10}K_{\text{M}(\text{Gp}, \text{H}_{-1})}$ due to the contribution of two deprotonated amides in GGG in



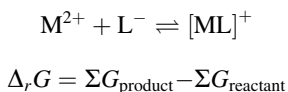
Scheme 1 Influence of **a** protonated and **b** deprotonated amide nitrogen of peptide bond on complex stability

Table 2 Influence of amide nitrogen in the peptide bond on stability of metal–glycine peptide complexes

| Metal ions | $\Delta \log_{10} \beta_{MGP}$ | | | $\Delta \log_{10} K_{M(Gp,H-1)}$ | $\Delta \log_{10} K_{M(Gp,H-2)}$ |
|------------------|--------------------------------|--------|-------|----------------------------------|----------------------------------|
| | GG–G | GGG–GG | GGG–G | GG–G | GGG–G |
| Fe ³⁺ | –2.07 | –0.24 | –2.31 | 0.56 | 0.72 |
| Cr ³⁺ | –1.59 | –0.03 | –1.62 | 0.51 | 1.02 |

which metal ions and GGG complexes form three five-membered chelate rings, while in the metal ions and GG systems the complexes form two five-membered chelate rings via nitrogen in the N-terminus, deprotonated amide nitrogen of the peptide and carboxyl in the C-terminus.

Contribution from the amide nitrogen to complex stability is further supported by the optimization and frequency analysis using Gaussian 09. From the geometry optimization, structures of the complexes that formed can be predicted (Fig. 2) and thermodynamic properties such as Gibbs energy (G) can be obtained from the frequency analysis. In this program, the complex equilibrium is presented as the Gibbs energy of reaction ($\Delta_r G$) that is calculated from the following relations:



where $\Delta_r G$ is proportional to the metal complex formation constant ($\log_{10} \beta$). Thus, according to this correlation, the more negative the $\Delta_r G$ value is, the larger the formation constant value will be and the complex formed will be more stable.

For each metal Hartree/particle ligand combination, Gaussian modeling was done by considering the possible binding sites that may contribute to complex formation. Values of $\Delta_r G$ for metal–ligand formation were calculated for the possible binding site of ligands and the one which shows the most negative value of $\Delta_r G$ (reported in Table 3) was chosen as the contributing binding site, and the structure of this complex will be used as the predicted structure of the formed complex. For example, in the case of the Fe³⁺–glycine complex, glycine may form a complex with the metal ion through its amine group and/or carboxyl group. During Gaussian geometry optimization and frequency calculations, Fe³⁺ was assumed to bind to glycine through its amine group only, through its carboxyl group only, and by chelate binding through both amine and carboxyl groups with the resulting $\Delta_r G$ of –0.320, –0.395 and –0.413 Hartree/particle, respectively. Hence glycine forms a complex and binds Fe³⁺ through its amine and carboxyl groups (as shown in Fig. 2a) and acts as a chelating ligand. Similarly, GG and GGG form chelates by their nitrogen and carbonyl oxygen, while gallic acid forms the most stable complex through its catechol site and ferulic acid forms the most stable complex through its carboxylate group.

From the calculated values of $\Delta_r G$ shown in Table 3, the negative $\Delta_r G$ and complex stability constant values decrease in the following order: $[M(GGG, H_{-2})] > [MGA]^- > [M(GG, H_{-1})]^+ > [M(GGG, H_{-1})]^+ > [MFA]^+ > [MG]^{2+} > [MGG]^{2+} > [MGGG]^{2+}$. The optimized geometry of $[M(GG, H_{-1})]^+$ and $[M(GGG, H_{-2})]$ (shown in Fig. 2c, f, respectively) and the calculated values of $\Delta_r G$, support the hypothesis that the deprotonated amide in GGG peptide forms three five-membered chelate rings with the metal ions, while in metal ion–GG system the complex forms two five-membered chelate rings via nitrogen in the N-terminus, deprotonated amide nitrogen of the peptide and carboxyl in the C-terminus.

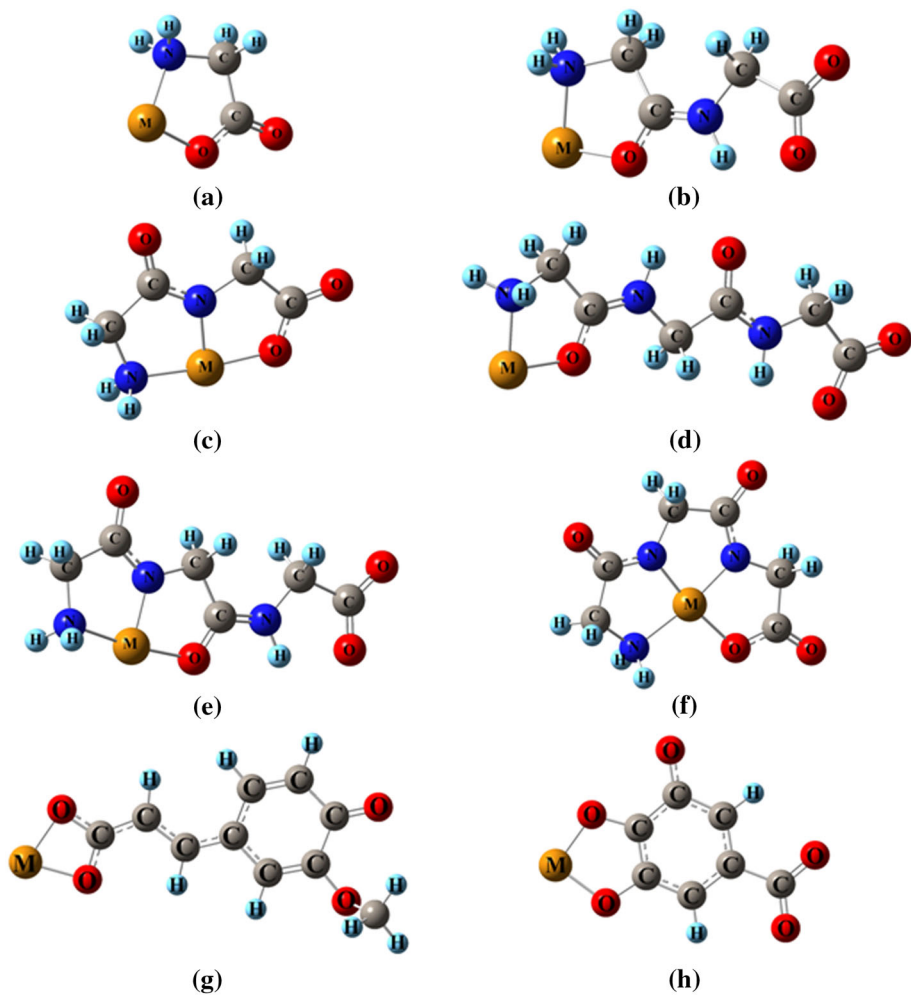


Fig. 2 Optimized structures of some complexes between trivalent metal ion (M) and glycine contained peptides: **a** $[MG]^{2+}$, **b** $[MGG]^{2+}$, **c** $[M(GG, H_{-1})]^+$, **d** $[MGGG]^{2+}$, **e** $[M(GGG, H_{-1})]^+$, **f** $[M(GGG, H_{-2})]$, **g** $[MFA]^+$, and **h** $[MGA]^-$; generated from Gaussian09 calculations

According to the Gaussian modeling result, it seems that GA has a more negative $\Delta_r G$ value than that of FA. This result is in agreement with the result obtained from potentiometric studies where the $\log_{10}\beta_{FeL}$ values are 22.97 and 11.48 when L is GA [36] and FA [37], respectively. This phenomenon may be due to formation of five-membered ring metal complexes in the case of GA while FA forms not-so-stable four-membered ring metal complexes with the bulkier side chain. On the other hand, FA has been shown to form a more stable complex with metal ion than G, GG and GGG. This phenomenon can be elucidated by the influence of charge and chelate effects on complex formation. For both Fe^{3+} and Cr^{3+} , the charge effect dominates over the chelate effect; thus the positively

Table 3 Gibbs energy ($\Delta_r G$) of complex formation obtained from optimization and frequency calculation by using the Gaussian 09 program

| Complex species | $\Delta_r G$ (Hartree/particle) | |
|------------------------------------|---------------------------------|--------|
| | M = Fe | M = Cr |
| Binary system | | |
| [MG] ²⁺ | -0.413 | -0.315 |
| [MGG] ²⁺ | -0.406 | -0.302 |
| [MGGH ₁] ⁺ | -0.515 | -0.393 |
| [MGGG] ²⁺ | -0.403 | -0.302 |
| [MGGGH ₁] ⁺ | -0.502 | -0.376 |
| [MGGGH ₂] | -0.613 | -0.517 |
| [MFA] ⁺ | -0.425 | -0.326 |
| [MGA] ⁻ | -0.605 | -0.511 |
| Mixed ligand system | | |
| [MFAG] | -0.584 | -0.493 |
| [MFAGG] | -0.547 | -0.456 |
| [MFAGGG] | -0.543 | -0.453 |
| [MGAG] ²⁻ | -0.668 | -0.560 |
| [MGAGG] ²⁻ | -0.625 | -0.545 |
| [MGAGGG] ²⁻ | -0.616 | -0.545 |

^a The calculation was done using the density functional theory (DFT)-B3LYP method combined with 6-31+G(d) as a basis set; 1 Hartree/particle = 2.626×10^3 kJ·mol⁻¹

charged Fe and Cr ions can attract the more negative charged ferulic acid and form metal–ligand complexes.

3.2 Formation of Mixed Ligand Complexes

Overall formation constants of FA and GA were acquired from previous research [36, 37]. These values, together with the overall formation constants of metal ions with G, GG and GGG, were introduced to the HYPERQUAD2008 program as constants and used for determination of mixed-ligand complex stability constants involving metal ions (M), glycine peptides (Gp) and phenolic acids (Ph). Representative potentiometric titration curves of Fe³⁺ with FA and G are shown in Fig. 3. The inflection in the ternary Fe–FA–G curve at moles NaOH added = 0.25 indicates complexation of Fe³⁺ with the deprotonated G since the inflection at this point is similar to the inflection of the G system (no metal) at moles NaOH added = 0.15, followed by the inflections at 0.30 and 0.35 which indicate attachment of the FA ligand to the Fe–G complex. With regard to the metal ions, an identical trend as for the binary system is observed in all systems, where Fe³⁺ forms a more stable complex than Cr³⁺ (Table 5). Moreover, in mixed-ligand systems containing GA, the complex is more stable than that containing FA and the stability of complexes ($\log_{10}\beta$) decreases in the following order of ligands GA–G > GA–GG > GA–GGG > FA–G > FA–GG > FA–GGG. As shown in Table 3, this trend is also supported by the $\Delta_r G$ values of the mixed-ligand complexes which were obtained from Gaussian 09 modeling. A more negative $\Delta_r G$ value indicates a more stable complex.

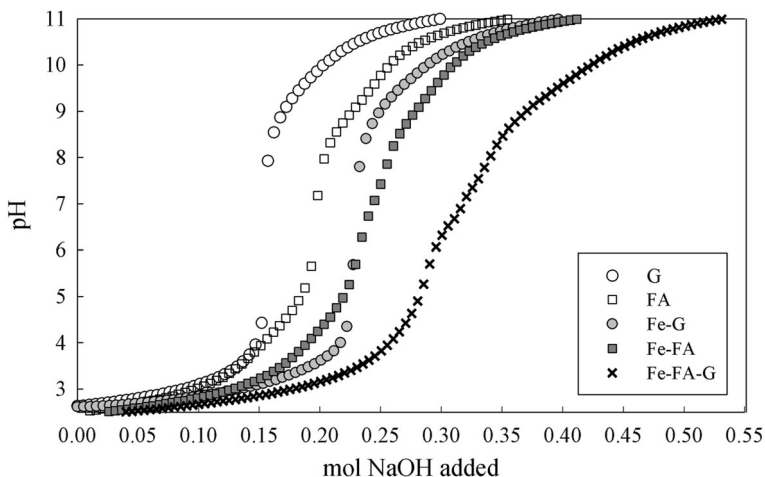


Fig. 3 Potentiometric titration curve, represented by FA for Fe^{3+} and G for the ligand

To investigate the stability of the mixed-ligand complexes relative to their corresponding binary complexes, $\Delta \log_{10} K$ values were calculated using the following equation [45]:

$$\Delta \log_{10} K = \log_{10} \beta_{\text{MGpPh}} - \log_{10} \beta_{\text{MGp}} - \log_{10} \beta_{\text{MPH}}$$

The calculated values of $\Delta \log_{10} K$ are given in Tables 4 and 5. The trend of $\Delta \log_{10} K$ values for both metal ions is opposite to the stability constant trend described above for the binary systems. For example, Fe^{3+} has higher stability constant values than that of Cr^{3+} in binary systems, but it yields more negative $\Delta \log_{10} K$ values than those of Cr^{3+} . This phenomenon can be explained based on the metal–ligand interaction behavior in binary and mixed ligand systems. If the interaction between a metal ion and a particular ligand to form a binary complex is strong, then it becomes difficult for another ligand to bind to the ligand–metal complex and form a mixed ligand complex, thus resulting in a negative $\Delta \log_{10} K$ value. These negative values also may be the result of reduction in the coordination sites of the metal ion, steric hindrance and the electrostatic effect [46–48].

From the obtained equilibrium constants, species distribution diagrams of the complex species formed can be illustrated as a function of pH by the HYSS2009 program. In Fig. 4, are presented typical species distribution diagrams of Fe^{3+} with mixed ligands FA and the glycine peptides. In all of the FA–G, FA–GG and FA–GGG diagrams, it can be seen that that mixed ligand complex species such as $[\text{FeFAGH}]$, $[\text{FeFAG}]$, $[\text{FeFAGG}]$, $[\text{FeFA}(\text{GG}, \text{H}_{-1})]$, $[\text{FeFAGGG}]$ and $[\text{FeFA}(\text{GGG}, \text{H}_{-2})]$ predominate. A closer look at these diagrams reveals that there is competition between FA and glycine since these two ligands have similar complexing ability towards trivalent metal ions. As shown in Fig. 4a, initially at pH 2, more than 60 % of Fe^{3+} exists as $[\text{Fe}(\text{FA}, \text{G}, \text{H})]$, 15 % as $[\text{FeG}]$ and 12 % as $[\text{FeFA}]$. Only less than 10 % of Fe^{3+} is left as free ion. As the pH is increased, $[\text{FeFAG}]$, $[\text{FeG}_2]$ and $[\text{FeFA}_2]$ start to form and, at approximately pH 6, nearly the same amounts of $[\text{FeFA}_2]$ (18 %) and $[\text{FeG}_2]$ (19 %) are formed. Similarly, for the Fe-FA-GG system, initially at pH 2, 59 % of the Fe^{3+} exists as $[\text{FeFA}]$ and 15 % as $[\text{FeGG}]$. At pH 7, more than 50 % of the complex species is $[\text{FeFAGG}]$ and the amount of this species decreases

Table 4 Overall formation constants of metal on (M)–glycine peptide (Gp)–ferulic acid (FA) complexes at 298.15 K and 0.15 mol·dm⁻³ NaNO₃

| Species | M = Fe ³⁺ | | M = Cr ³⁺ | |
|---------------------------------------|----------------------------|----------------------|----------------------------|----------------------|
| | log ₁₀ β ± S.D. | Δlog ₁₀ K | log ₁₀ β ± S.D. | Δlog ₁₀ K |
| Gp = G | | | | |
| σ ^{*a} | 1.103 | | 1.017 | |
| [MGpFA] | 20.07 ± 0.04 | -2.10 | 15.87 ± 0.03 | -1.09 |
| [MGpFAH] ⁺ | 24.49 ± 0.07 | | | |
| Gp = GG | | | | |
| σ ^{*a} | 1.157 | | 1.099 | |
| [MGpFA] | 19.25 ± 0.04 | -0.85 | 15.15 ± 0.08 | -0.22 |
| [MGpFAH] ⁺ | | | 21.02 ± 0.04 | |
| [MGpFAH ₋₁] ⁻ | 12.52 ± 0.04 | | 9.64 ± 0.04 | |
| Gp = GGG | | | | |
| σ ^{*a} | 1.242 | | 1.009 | |
| [MGpFA] | 18.06 ± 0.02 | -1.80 | 14.91 ± 0.03 | -0.43 |
| [MGpFAH] ⁺ | | | 21.36 ± 0.03 | |
| [MGpFAH ₋₁] ⁻ | 10.55 ± 0.04 | | 9.8 ± 0.03 | |
| [MGpFAH ₋₂] ²⁻ | 3.17 ± 0.03 | | 2.23 ± 0.03 | |

^a Sigma* (σ^{*}) is the goodness of fit for a system with ±95 % probability

Table 5 Overall formation constants of metal ion (M)–glycine peptide (Gp)–gallic acid (GA) complexes at 298.15 K and 0.15 mol·dm⁻³ NaNO₃

| Species | M = Fe ³⁺ | | M = Cr ³⁺ | |
|---------------------------------------|----------------------------|----------------------|----------------------------|----------------------|
| | log ₁₀ β ± S.D. | Δlog ₁₀ K | log ₁₀ β ± S.D. | Δlog ₁₀ K |
| Gp = G | | | | |
| σ ^{*a} | 1.091 | | 1.106 | |
| [MGpGA] ²⁻ | 29.08 ± 0.06 | -4.58 | 24.85 ± 0.02 | -4.42 |
| [MGpGAH] ⁻ | 37.36 ± 0.06 | | | |
| [MGpGAH ₂] | 43.38 ± 0.06 | | | |
| Gp = GG | | | | |
| σ ^{*a} | 1.057 | | 1.013 | |
| [MGpGA] ²⁻ | 26.69 ± 0.03 | -4.90 | 23.10 ± 0.03 | -4.58 |
| [MGpGAH] ⁻ | 33.72 ± 0.08 | | 30.94 ± 0.03 | |
| [MGpGAH ₋₁] ³⁻ | 18.12 ± 0.02 | | 14.33 ± 0.04 | |
| Gp = GGG | | | | |
| σ ^{*a} | 1.075 | | 1.089 | |
| [MGpGA] ²⁻ | 25.95 ± 0.03 | -5.40 | 23.31 ± 0.02 | -5.34 |
| [MGpGAH] ⁻ | | | 30.18 ± 0.02 | |
| [MGpGAH ₂] | | | 36.12 ± 0.03 | |
| [MGpGAH ₋₁] ³⁻ | 17.54 ± 0.01 | | 13.42 ± 0.02 | |
| [MGpGAH ₋₂] ⁴⁻ | 6.00 ± 0.05 | | 1.79 ± 0.06 | |

^a Sigma* (σ^{*}) is the goodness of fit for a system with ±95 % probability

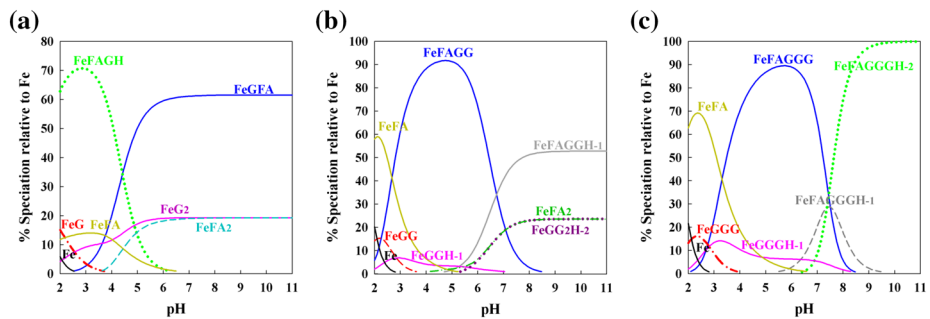


Fig. 4 The species distribution curves of **a** Fe^{3+} -G-FA, **b** Fe^{3+} -GG-FA, **c** Fe^{3+} -GGG-FA at $T = 298.15 \text{ K}$, $I = 0.15 \text{ mol}\cdot\text{dm}^{-3} \text{ NaNO}_3$ and $[\text{M}:\text{Gp}:\text{Ph}] 1:1:1$. Charges are omitted for simplicity

with increasing pH. At pH above 8, the major species in this system is $[\text{FeFA}(\text{GG},\text{H}_{-1})]$ (53 %) with the other two species $[\text{FeFA}_2]$ and $[\text{Fe}(\text{GG}_2,\text{H}_{-2})]$ being found in equal amounts (23.5 %).

4 Conclusion

In this work, interactions between trivalent ions (Fe^{3+} and Cr^{3+}), glycine peptides (G, GG and GGG) and phenolates (FA and GA) were studied at 298.15 K and ionic strength $0.15 \text{ mol}\cdot\text{dm}^{-3} \text{ NaNO}_3$ by using the pH-potentiometry technique. The complex stability constants, as overall formation constants ($\log_{10}\beta_{pqrs}$), were obtained by the HYPER-QUAD2008 program. In terms of the ligands, the stability constant of the complexes in binary systems decreases in the following order $\text{GA} > \text{FA} > \text{G} > \text{GG} > \text{GGG}$. Among the glycine peptides, the longer the linear carbon side chain is, the greater is the steric effect and thus the complex formed is less stable. From investigation of the contribution of deprotonated or undeprotonated amide peptides to stability constants, it was found that the deprotonated amide nitrogen in the peptide backbone participated in complex formation thus it enhanced the complex's stability. The stability constants of complexes in both binary and mixed-ligand systems show the same trend, where Fe^{3+} forms a more stable complex with ligands than Cr^{3+} . Based on its $\log_{10}\beta$ values, the mixed-ligand complexes formed are more stable than the corresponding binary complexes. Moreover, the mixed-ligand complex containing GA is more stable than that containing FA. In mixed-ligand systems, the stability of complexes decreases in the following order of ligands: $\text{GA-G} > \text{GA-GG} > \text{GA-GGG} > \text{FA-G} > \text{FA-GG} > \text{FA-GGG}$.

Acknowledgments Financial supports by the National Science Council of Taiwan (NSC 102-2221-E-011-079) and National Taiwan University of Science and Technology (101H451403) are greatly appreciated. The authors thank to Prof. Jiang Jyh-Chiang for his valuable suggestions regarding the Gaussian Program.

References

1. Irwin, R.J.: Environmental Contaminants Encyclopedia: Chromium III (Trivalent Chromium) Entry. National Park Service, Water Resources Division, Fort Collins (1997)
2. Grevat, P.C.: Toxicological Review of Trivalent Chromium. U.S. Environmental Protection Agency, Washington, DC (1998)

3. Khade, B.C., Deore, P.N., Arbad, B.R.: Composition and stability of chromium metal complexes with drug salbutamol and amino acid. *Pharma Sci. Monitor.* **2**, 73–86 (2011)
4. Cotton, F.A., Wilkinson, G.: *Advanced Inorganic Chemistry. A Comprehensive Text*, 4th edn. Wiley, New York (1980)
5. Faa, G., Crisponi, G.: Iron chelating agents in clinical practice. *Coord. Chem. Rev.* **184**, 291–310 (1999)
6. Papanikolaou, G., Pantopoulos, K.: Iron metabolism and toxicity. *Toxicol. App. Pharm.* **202**, 199–211 (2005)
7. Muir, A., Hopfer, U.: Regional specificity of iron uptake by small intestinal brush-border membranes from normal and iron-deficient mice. *Am. J. Physiol.* **248**, 376–379 (1985)
8. Nelson, L.S., Lewin, N.A., Howland, M.A., Hoffman, R.S., Goldfrank, L.R., Flomenbaum, N.E.: *Goldfrank's Toxicological Emergencies*, 8th edn. McGraw-Hill, New York (2008)
9. Flora, S.J.S., Pachauri, V.: Chelation in metal intoxication. *Int. J. Environ. Res. Public Health* **7**, 2745–2788 (2010)
10. Rogan, W.J., Dietrich, K.N., Ware, J.H., Dockery, D.W., Salganik, M., Radcliffe, J., Jones, R.L., Ragan, N.B., Chisolm, J.J.J., Rhoads, G.G.: The effect of chelation therapy with succimer on neuropsychological development in children exposed to lead. *New Eng. J. Med.* **344**, 1421–1426 (2001)
11. May, M.E., Hill, J.O.: Energy content of diets of variable amino acid composition. *Am. J. Clin. Nutr.* **52**, 766–770 (1990)
12. Sigel, H., Martin, R.B.: Coordinating properties of the amide bond. Stability and structure of metal ion complexes of peptides and related ligands. *Chem. Rev.* **82**, 385–426 (1981)
13. Brown, J.A., Khodr, H., Hider, R.C., Rice-Evans, C.: Structural dependence of flavonoid interactions with Cu^{2+} ions: implications for their antioxidant properties. *Biochem. J.* **330**, 1173–1178 (1998)
14. Srinivasan, M., Sudheer, A.R., Menon, V.P.: Ferulic acid: therapeutic potential through its antioxidant property. *J. Clin. Biochem. Nutr.* **40**, 92–100 (2006)
15. Soobrattee, M.A., Neergheen, V.S., Luximon-Ramma, A., Aruoma, O.I., Bahorun, T.: Phenolics as potential anti-oxidant therapeutic agents: mechanism and actions. *Mutat. Res.* **579**, 200–213 (2005)
16. Zhou, B., Jia, Z.-S., Chen, Z.-H., Yang, L., Wu, L.-M., Liu, Z.-L.: Synergistic antioxidant effect of green tea polyphenols with α -tocopherol on free radical initiated peroxidation of linoleic acid in micelles. *J. Chem. Soc. Perkin Trans.* **2**, 785–791 (2000)
17. Zhang, H.-M., Wang, C.-F., Liu, Z.-M., Wang, Y.-Y., Du, S.-S., Shen, S.-M., Wang, G.-L., Liu, P., Deng, Z.-W., Liu, Z.-L.: Antioxidant phenolic compounds from Pu-erh tea. *Molecules* **17**, 14037–14045 (2012)
18. Mertz, C., Brat, P., Cheynier, V., Guenard, Z.: Analysis of phenolic compounds in two blackberry species (*Rubus glaucus* and *Rubus adenotrichus*) by high-performance liquid chromatography with diode array detection and electrospray ion trap mass spectrometry. *J. Agric. Food Chem.* **55**, 8616–8624 (2007)
19. Ohashi, H., Yamamoto, E., Lewis, N.G., Towers, G.H.N.: 5-Hydroxyferulic acid in zeae mays and hordeum vulgare cell walls. *Phytochemistry* **26**, 1915–1916 (1987)
20. Teuchy, H., Van-Sumere, C.F.: The metabolism of (1- ^{14}C) phenylalanine, (3- ^{14}C) cinnamic acid and (2- ^{14}C) ferulic acid in the rat. *Arch. Int. Physiol. Biochim.* **79**, 589–618 (1971)
21. Adam, A., Crespy, V., Levrat-Verny, M.A., Leenhardt, F., Leuillet, M., Demigne, C., Remesy, C.: The bioavailability of ferulic acid is governed primarily by the food matrix rather than its metabolism in intestine and liver in rats. *J. Nutr.* **132**, 1962–1968 (2002)
22. Graf, E.: Antioxidant potential of ferulic acid. *Free Radic. Biol. Med.* **13**, 435–448 (1992)
23. Fujimaki, M., Tsugita, T., Kurata, T.: Fractionation and identification of volatile acids and phenols in the steam distillate of rice bran. *Agric. Biol. Chem.* **41**, 1721–1725 (1977)
24. Inoue, M., Suzuki, R., Sakaguchi, N., Li, Z., Takeda, T.: Selective induction of cell death in cancer cells by gallic acid. *Biol. Pharm. Bull.* **18**, 1526–1530 (1995)
25. Frisch, M.J., Trucks, G.W., Schlegel, H.B., Scuseria, G.E., Robb, M.A., Cheeseman, J.R., Scalmani, G., Barone, V., Mennucci, B., Petersson, G.A., Nakatsuji, H., Caricato, M., Li, X., Hratchian, H.P., Izmaylov, A.F., Bloino, J., Zheng, G., Sonnenberg, J.L., Hada, M., Ehara, M., Toyota, K., Fukuda, R., Hasegawa, J., Ishida, M., Nakajima, T., Honda, Y., Kitao, O., Nakai, H., Vreven, T., Montgomery, J.J.A., Peralta, J.E., Ogliaro, F., Bearpark, M., Heyd, J.J., Brothers, E., Kudin, K.N., Staroverov, V.N., Kobayashi, R., Normand, J., Raghavachari, K., Rendell, A., Burant, J.C., Iyengar, S.S., Tomasi, J., Cossi, M., Rega, N., Millam, J.M., Klene, M., Knox, J.E., Cross, J.B., Bakken, V., Adamo, C., Jaramillo, J., Gomperts, R., Stratmann, R.E., Yazyev, O., Austin, A.J., Cammi, R., Pomelli, C., Ochterski, J.W., Martin, E.L., Morokuma, K., Zakrzewski, V.G., Voth, G.A., Salvador, P., Dannenberg, J.J., Dapprich, S., Daniels, A.D., Farkas, O., Foresman, J.B., Ortiz, J.V., Cioslowski, J., Fox, D.J.: *Gaussian 09*, revision A.1. 2009. Gaussian, Inc.: Wallingford CT (2009)
26. Gans, P., O'Sullivan, B.: GLEE, a new computer program for glass electrode calibration. *Talanta* **51**, 33–37 (2000)

27. House, J.E.: Inorganic Chemistry, 1st edn. Academic Press/Elsevier (2008)
28. Becke, A.D.: Density-functional thermochemistry. III. The role of exact exchange. *J. Chem. Phys.* **98**, 5648–5652 (1993)
29. Lee, C., Yang, W., Parr, R.G.: Development of the Colle–Salvetti correlation-energy formula into a functional of the electron density. *Phys. Rev. B* **37**, 785–789 (1998)
30. Rassolov, V.A., Pople, J.A., Ratner, M.A., Windus, T.L.: 6-31G* basis set for atoms K through Zn. *J. Chem. Phys.* **109**, 1223–1229 (1998)
31. Ramos, J.M., Versiane, O., Felcman, J., Téllez Soto, C.A.: Fourier transform infrared spectrum, vibrational analysis and structural determination of the trans-bis(glycine)nickel(II) complex by means of the RHF/6-311G and DFT:B3LYP/6-31G and 6-311G methods. *Spectrochim. Acta Part A* **68**, 1370–1378 (2007)
32. Ramos, J.M., Versiane, O., Felcman, J., Téllez Soto, C.A.: FT-IR vibrational spectrum and DFT: B3LYP/6-31G and B3LYP/6-311G structure and vibrational analysis of glycinate-guanidoacetate nickel(II) complex: [Ni(Gly)(Gaa)]. *Spectrochim. Acta Part A* **72**, 182–189 (2009)
33. Chachkov, D.V., Mikhailov, O.V.: DFT B3LYP calculation of the spatial structure of Co(II), Ni(II), and Cu(II) template complexes formed in ternary systems metal(II) ion–dithiooxamide–formaldehyde. *Russ. J. Inorg. Chem.* **54**, 1952–1956 (2009)
34. Kawakami, J., Miyamoto, R., Fukushi, A., Shimozaki, K., Ito, S.: Ab initio molecular orbital study of the complexing behavior of *N*-ethyl-1-naphthalenecarboxamide as fluorescent chemosensors for alkali and alkaline earth metal ions. *J. Photochem. Photobiol. A* **146**, 163–168 (2002)
35. Angkawijaya, A.E., Fazary, A.E., Ismadji, S., Ju, Y.-H.: Cu(II), Co(II), and Ni(II)—antioxidative phenolate–glycine peptide systems: an insight into its equilibrium solution study. *J. Chem. Eng. Data* **57**, 3443–3451 (2012)
36. Hernowo, E.: Stability Constant Study: First Transition Metal Ions with Biological Important Ligands; Gallic Acid, *L*-Norleucine and Nicotinic Acid. LAP LAMBERT Academic Publishing, Germany (2011)
37. Angkawijaya, A.E., Fazary, A.E., Hernowo, E., Taha, M., Ju, Y.-H.: Iron(III), chromium(III), and copper(II) complexes of *L*-norvaline and ferulic Acid. *J. Chem. Eng. Data* **56**, 532–540 (2011)
38. Pettit, L.D., Powell, K.J.: A Comprehensive Database of Published Data on Equilibrium Constants of Metal Complexes and Ligands. IUPAC and Academic Software (2001)
39. Hong, C.-P., Kim, D.-W., Choi, K.-Y., Kim, C.-T., Choi, Y.G.: Stability constants of first-row transition metal and trivalent lanthanide metal ion complexes with macrocyclic tetraazatetraacetic and tetraaza-tetramethylacetic acids. *Bull. Korean Chem. Soc.* **20**, 297–300 (1999)
40. Brunetti, A.P., Lim, M.C., Nancollas, G.H.: Thermodynamics of ion association. XVII. Copper complexes of diglycine and triglycine. *J. Am. Chem. Soc.* **90**, 5120–5126 (1968)
41. Pagenkopf, G.K., Margerum, D.W.: Proton-transfer reaction with copper(II)–triglycine (CuH-2L[−]). *J. Am. Chem. Soc.* **90**, 501–502 (1968)
42. Martin, R.B., Chamberlin, M., Edsall, J.T.: The association of nickel(II) ion with peptides. *J. Am. Chem. Soc.* **82**, 495–498 (1960)
43. Basolo, F., Chen, Y.T., Murmann, R.K.: Steric effects and the stability of complex compounds. IV. The chelating tendencies of *c*-substituted ethylenediamines with copper(II) and nickel(II) ions. *J. Am. Chem. Soc.* **76**, 956–959 (1954)
44. Lenarcik, B., Kierzkowska, A.: The Influence of alkyl chain length and steric effect on stability constants and extractability of Zn(II) complexes with 1-alkyl-4(5)-methylimidazoles. *Sep. Sci. Technol.* **39**, 3485–3508 (2004)
45. Sigel, H., Prijs, B., Martin, R.B.: Stability of binary and ternary β-alanine containing dipeptide copper(II) complexes. *Inorg. Chim. Acta* **56**, 45–49 (1981)
46. Turkel, N., Sahin, C.: Stability of binary and ternary copper(II) complexes with 1,10-phenanthroline, 2,2′-bipyridyl and some α-amino acids in aqueous medium. *Chem. Pharm. Bull.* **57**, 694–699 (2009)
47. Khade, B.C., Deore, P.M., Arbad, B.R.: Mixed-ligand complex formation of copper(II) with some aminoacids and drug dapsone. *Int. J. ChemTech. Res* **2**, 1036–1041 (2010)
48. Lozano, M.J., Borrás, J.: Antibiotic as ligand. Coordinating behavior of the cephalixin towards Zn(II) and Cd(II) ions. *J. Inorg. Biochem.* **31**, 187–195 (1987)
49. Khalil, M.M., Fazary, A.E.: Potentiometric studies on binary and ternary complexes of di- and trivalent metal ions involving some hydroxamic acids, amino acids, and nucleic acid components. *Monatsh. Chem.* **135**, 1455–1474 (2004)